



Evaluating of Parotid Gland Tumours According to Diffusion Weighted MRI

Çınar Balçık, Hüseyin Akan, Lütfi İncesu

ABSTRACT

The aim of this study is evaluating the contribution of diffusion-weighted MR imaging (DWI) in the final diagnosis of patient that parotid gland tumours has been determined. Forty patients with 41 parotid masses were included to this study. The mean Apparent Diffusion Coefficient (ADC) values were calculated for all of lesions by performing DWI. 28 benign and 13 malignant tumours were detected as a final diagnosis. ADC values of these lesions were compared. The optimal cutoff ADC value was determined for discrimination of these lesions by using ROC curve analysis. The most often benign and malignant tumours of parotid gland were pleomorphic adenoma and secondary tumours, respectively. The highest ADC value as $2.10 \pm 0.26 \times 10^{-3} \text{ mm}^2/\text{sec}$ was belong to pleomorphic adenoma. The mean ADC value of pleomorphic adenoma was significantly higher than other lesions. As a result of ROC curve analysis, pleomorphic adenomas were differentiated from all other benign and malignant tumours with $1.60 \times 10^{-3} \text{ mm}^2/\text{sec}$ cutoff ADC value that had sensitivity of 94.7% and specificity of 100%; and also malignant tumours were differentiated from Warthin's tumours with $1.01 \times 10^{-3} \text{ mm}^2/\text{sec}$ cutoff ADC value that had sensitivity of 92.3% and specificity of 100%. We could differentiated pleomorphic adenomas, Warthin tumours and malignant tumours each other which are the most common parotid gland tumours by using the value of ADC.

Key words: Parotid gland, pleomorphic adenoma, magnetic resonance imaging, diffusion, ADC

Parotis Bezi Tümörlerinin Difüzyon Ağırlıklı MRG ile Değerlendirilmesi

ÖZET

Bu çalışmanın amacı, parotis bezi tümörü saptanan olgularda difüzyon ağırlıklı MRG (DAG)'nin son tanıya katkısını değerlendirmektir. Çalışmaya parotis bezinde toplam 41 lezyonu olan 40 hasta alındı. Tüm hastalara DAG yapılarak tüm lezyonların ortalama görünen difüzyon katsayısı (ADC) değerleri hesaplandı. Son tanıya göre 28 tane benin, 13 tane malin lezyon saptandı. Bu lezyonların ADC değerleri karşılaştırıldı. Ayrıca lezyonları ayırt etmek için ROC eğri analizi kullanılarak optimal cutoff ADC değerleri bulundu. Parotis bezinin en sık benin ve malin tümörleri sırasıyla pleomorfik adenom ve sekonder tümörler idi. En yüksek ADC değeri $2.10 \pm 0.26 \times 10^{-3} \text{ mm}^2/\text{sn}$ ile pleomorfik adenomlara aitti. Pleomorfik adenomların ortalama ADC değeri diğer lezyonlardan anlamlı olarak yüksekti. ROC eğri analizi sonuçlarına göre pleomorfik adenom, diğer tüm benin ve malin tümörlerden $1.60 \times 10^{-3} \text{ mm}^2/\text{sn}$ cutoff ADC değeri ile %94.7 duyarlılık ve %100 özgüllükle; malin tümörler, Whartin tümöründen ise $1.01 \times 10^{-3} \text{ mm}^2/\text{sn}$ cutoff ADC değeri ile %92.3 duyarlılık ve %100 özgüllükle ayırt edildi. Biz çalışmamızda en sık görülen parotis bezi tümörleri olan pleomorfik adenom, Warthin tümörü ve malin tümörleri ADC değerlerini kullanarak ayırdık.

Anahtar kelimeler: Parotis bezi, pleomorfik adenom, manyetik rezonans görüntüleme, difüzyon, ADC

INTRODUCTION

Magnetic resonance imaging (MRI) has been sensitized to the microscopic motions of water molecules on the tissue by means of technological developments, so diffusion weighted MRI (DWI) has been started to perform. Thus, the density and motion of water molecules on the tissue might be evaluated and water balance between intracellular and extracellular compartment might be showed. The apparent diffusion coefficient (ADC) of lesions has been calculated by DWI and the diffusion could be calculated quantitatively by means of acquired ADC values. The ADC specifies special diffusion capacity of a biological tissue (1,2). In the previous studies, direct relationship between ADC value and tumor cellularity was showed. Initially, this feature has invented an application area in the differential diagnosis of the intracranial masses. Then, extended application area including head-neck (3,4,5), breast (6), vertebral column (7), musculoskeletal system (8), abdomen and pelvis (9) were appeared in the subsequent years.

In this study, we aimed to calculate ADC values for differentiation of the lesions as benign or malignant and classification benign ones themselves in the patient that parotid gland tumors has been determined.

MATERIALS AND METHODS

Subjects

Forty patients with parotid gland tumor of whom DWI had been performed were investigated retrospectively by use of our hospital database. After the approval from the local ethics committee of our hospital.

Conventional MRI Protocol

Routine parotid gland MRI was performed by using a 1.5 T magnetik rezonans imager (Siemens Magnetom Symphony Quantum, Erlangen, Germany) with a head coil. Routine examination sequences were consist of T1 weighted TSE axial (TR / TE: 445 ms / 11 ms, thickness: 5 mm, FOV: 230 mm, matrix 157 x 256, average: 2), T2 weighted TSE axial (TR / TE: 4480 ms / 108 ms, thickness: 5 mm, FOV: 230 mm, matrix 199 x 384, average: 2), T2 weighted TSE coronal with fat suppression (TR / TE: 4460 ms / 103 ms, thickness: 4 mm, FOV: 279 mm, matrix 144 x 256, average: 2), T1 weighted TSE with fat

suppression and intravenous contrast axial and coronal (TR / TE: 557 ms / 15 ms, thickness: 4 mm, FOV: 280 mm, matrix 192 x 256, average: 1).

Diffusion Weighted MRI Protocol

DWI had been performed before enhanced imagings. The b values were 0, 500 and 1000 s/mm². The technical parameters were TR / TE: 3400 ms / 94 ms, thickness: 5 mm, FOV: 230 mm, matrix: 128 x 128, bandwidth: 1346 Hz / pixel, average: 3, scan time: 76 s, distance factor 30%. DWI sequences were obtained by using diffusion sensitive gradients to axial projection SSEP-SE T2 on three directions (x,y,z) with different b values (0, 500 and 1000 s/mm²). While the initial series on imaging group of sequence obtained from EP-SE T2 (b=0, no diffusion gradient), subsequent two series arise from images that performed diffusion sensitive gradients with the b value 500 s/mm² and b value 1000 s/mm² on x, y, z directions to the initial series. Isotropic images were composed of images that multiplied by two and got cubic root of measured signal intensity on x, y, z directions which were created by equipment. The ADC maps relating to isotropic images of b value 500 s/mm² and 1000 s/mm² were constituted by equipment automatically and ADC value of all lesions were measured from these maps.

Image Analysis

All DWI groups were transferred work station (Leonardo konsol, software version 2.0; Siemens; GERMANY) to get ADC measurement. Before the ADC measurement had been performed, the location of the lesions were detected by analysing DWI which obtained b value 500 s/mm² and 1000 s/mm². Moreover, restricted or increased areas on the lesion were detected by qualitatively analysed ADC maps. The ADC measurements were performed by regio of interested in (ROI) that had been located on each parotid lesion at the ADC maps. ROI was circular and the surface area was 0.7 cm² for each lesion. The ADC measures were performed from homogeneous solid regions that had restricted diffusion area; if not performed from solid regions that had increased diffusion area. If the lesions had heterogeneous structure, the measurements were performed from solid areas (which determined on conventional sequences and/or enhanced areas on sequences with contrast media).

Besides, the ADC measurements were obtained from the sites of cystic necrotic regions which tumours had.

Statistical Analysis

The parotid gland tumors were classified as benign or malignant masses. Additionally, all benign lesions were classified among themselves according to the final diagnosis too. All statistical analyses were performed with the Statistical Package for Social Sciences, 15.0 (SPSS). Age and ADC values were showed as “mean \pm standard deviation (SD)”. The groups which wanted to compare the variabilities was classified as “benign or malignant lesion”, “subtypes of benign lesion” and “pleomorphic adenoma, Warthin’s tumor or malignant lesion”. For ADC value, Kruskal Wallis test was used for comparisons of within majority groups and Mann-Whitney U test was used for comparisons of dual group. The optimal cutoff ADC value was determined for discriminating pleomorphic adenoma from all benign and malignant tumours; malignant tumours from Warthin’s tumours by using ROC curve analysis.

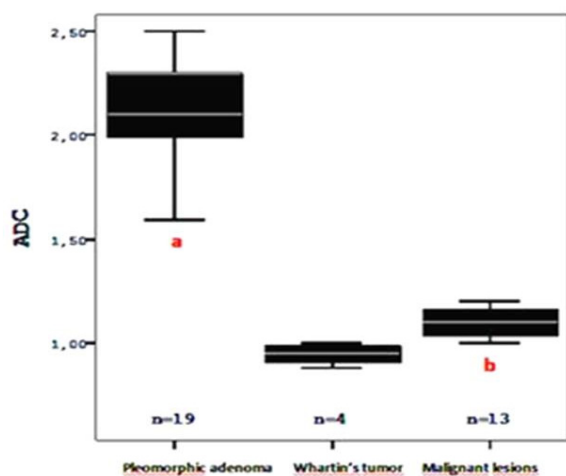


Figure 1. ADC value of pleomorphic adenoma, Warthin’s tumour and malignant lesions. a) ADC value of group 1 is significantly higher than group 2 ($p < 0.001$) and group 3 ($p < 0.001$). b) ADC value of group 3 is significantly higher than group 2 ($p = 0.001$)

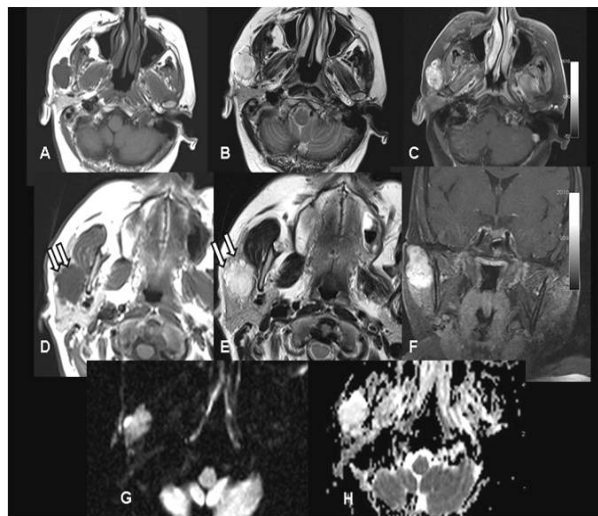


Figure 2. 54 years old female patient. There is a mass on superficial lobe of right parotid gland had pronounced lobulated contour but mostly well defined; intense enhancing on coronal and axial enhanced image (F,C). Nevertheless, the irregular contour on anterior wall of the lesion (arrows) causes malignancy suspicion (D, E). The hyperintensity on DWI (G) is because of T2 shine-through. ADC value of lesion was calculated as $2.1 \times 10^{-3} \text{ mm}^2/\text{sec}$ on the ADC map (H). The irregular contour on anterior wall of the lesion that recognised as pleomorphic adenoma with histopathologically was reported as capsule invasion.

The sensitivity, the specificity and the area under curve were calculated with confidence interval (CI) of 95% for DWI. $p < 0.05$ was considered to indicate statistical significance.

RESULTS

Total 41 parotid gland masses in the 40 patients (22 females, 18 males; age ranging between 16-85 years; mean age, 51.5 ± 19.1 years) were included to this study. Six of these had been diagnosed by histopathological examination of fine needle aspiration biopsies (FNAB), 33 surgical biopsies and one incisional biopsy was examined. One mass (lipoma) had been diagnosed via pathognomonic MRI and CT features.

Pathological diagnosis of these lesions were pleomor-

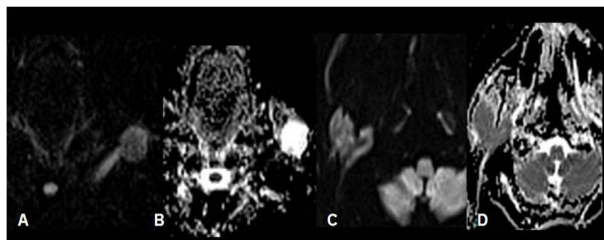


Figure 3. 67 years old female patient with pleomorphic adenoma (A,B) and 69 years old female patient with carcinoma ex pleomorphic adenoma. The carcinoma ex pleomorphic adenoma is shown restricted diffusion that characterized by signal features of slightly hyperintense on diffusion weighted image (C), pronounced hypointense on ADC map (D). The ADC value of lesion was calculated as $1.2 \times 10^{-3} \text{ mm}^2/\text{sec}$. The ADC value of pleomorphic adenoma was calculated as $2.5 \times 10^{-3} \text{ mm}^2/\text{sec}$ that obtained with ADC map (B).

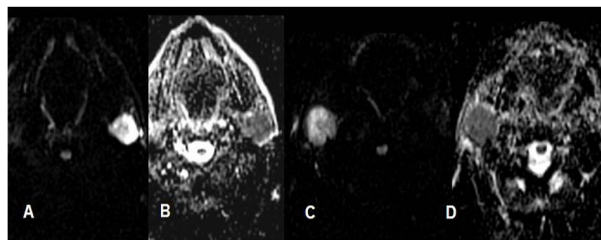


Figure 4. The Warthin's tumour (A,B) and mucoepidermoid carcinoma (C,D) are shown restricted diffusion samples. The ADC values were calculated as $0.88 \times 10^{-3} \text{ mm}^2/\text{sec}$ on first patient, $1.02 \times 10^{-3} \text{ mm}^2/\text{sec}$ on second one.

phic adenoma (Figure 2, 3a and 3b), Warthin's tumor (Figure 4a, 4b), basal cell adenoma, dermoid cyst, cyst that was full of keratinized material, lipoma, mucoepidermoid carcinoma (Figure 4c, 4d), adenoid cystic carcinoma, carcinoma of the salivary duct, adenocarcinoma, carcinoma ex-pleomorphic adenoma (Figure 3c and 3d), squamous cell carcinoma and secondary tumours. While, the most common benign parotid gland lesion was pleomorphic adenoma, secondary tumours were the most determined lesions within the malignant tumors.

No sex differences were found within 41 benign or malignant lesions. Mean age of malignant lesions was significantly higher than benign ones ($p=0.038$). The mean ADC value of benign lesions was measured as $1.74 \pm 0.58 \times 10^{-3} \text{ mm}^2/\text{sec}$, malignant ones was $1.13 \pm 0.13 \times 10^{-3} \text{ mm}^2/\text{sec}$ and the mean ADC values of benign lesions were significantly higher than malignant lesions ($p=0.006$).

Total 28 benign lesions were classified to subtypes and ADC values of them were compared (table 1). There was no significant difference in the case of age between the groups. Sex distribution and ADC values were significantly different ($p=0.024$ and $p=0.001$, respectively).

Dual group comparisons were performed after saw that there was difference between benign lesions's subtypes as to ADC values. As to this, the mean ADC values of pleomorphic adenomas were significantly higher than Warthin's tumors ($p<0.001$), basal cell adenomas ($p=0.010$), cystic lesions ($p=0.010$). There were not significantly difference between dual group comparisons except these.

Because of malignant lesion types had less number, they were not compared among themselves, the ADC values that belonging to each group were showed on Table 2.

In the dual comparisons were performed between pleo-

Table 1. Comparison of data between benign lesions according to subtypes

	Sex (M/F)	Age	ADC
Pleomorphic adenoma (n=19)	6/13	45.9±21.3	2.10±0.26
Warthin's tumor (n=4)	4/0	55.0±6.8	0.94±0.05
Basal cell adenoma (n=2)	2/0	47.0±0.0	1.29±0.04
Dermoid cyst or high density cyst (n=2)	0/2	45.5±13.4	0.85±0.03
Lipoma (n=1)	0/1	47.0	0.80
P	0.024	0.943	0.001

ADC=Apparent diffusion coefficient ($\times 10^{-3} \text{ mm}^2/\text{s} \pm \text{SD}$)

Table 2. ADC values of malignant parotid gland tumors

	Number	ADC
Mucoepidermoid carcinoma	1	1.02
Adenoid cystic carcinoma	1	1.53
Salivary duct carcinoma	1	1.03
Adenocarcinoma	1	1.00
Carcinoma ex-pleomorphic adenoma	3	1.14±0.09
Squamous cell carcinoma	2	1.11±0.02
Secondary tumors	4	
Metastasis of infiltrative ductal breast cancer	1	1.09
Infiltration of squamous cell carcinoma	2	1.15±0.00
Infiltration of basal cell carcinoma	1	1.10

ADC=Apparent diffusion coefficient ($\times 10^{-3} \text{ mm}^2/\text{s} \pm \text{SD}$)

morphic adenoma (group 1), Warthin's tumour (group 2) and malignant tumours (group 3). The ADC values of the pleomorphic adenoma were significantly higher than malignant tumours ($p < 0.001$) or Warthin's tumours ($p = 0.001$). The ADC values of malignant tumours were significantly higher than Warthin's tumours ($p = 0.001$) (Figure 1).

The optimal cutoff ADC values were determined by using ROC curve analysis. Accordingly, the pleomorphic adenomas were differentiated from all other benign and malignant tumours with $1.60 \times 10^{-3} \text{ mm}^2/\text{sec}$ cutoff ADC value that had sensitivity of 94.7% (18/19, 95% CI) and specificity of 100% (22/22, 95% CI). The pleomorphic adenomas were differentiated from Warthin's tumours with $1.60 \times 10^{-3} \text{ mm}^2/\text{sec}$ cutoff ADC value that had sensitivity of 94.7% (18/19, 95% CI) and specificity of 100% (4/4, 95% CI). And also the pleomorphic adenomas were differentiated from malignant tumours with $1.60 \times 10^{-3} \text{ mm}^2/\text{sec}$ cutoff ADC value that had sensitivity of 94.7% (18/19, 95% CI) and specificity of %100 (13/13, %95 CI); the malignant tumours were differentiated from Warthin's tumours with $1.01 \times 10^{-3} \text{ mm}^2/\text{sec}$ cutoff ADC value that had sensitivity of 92.3% (12/13, 95% CI) and specificity of 100% (4/4, 95% CI).

DISCUSSION

Not only distinguishing between benign or malignant lesions but also determining the definite histological subtypes of primary tumours of parotid gland is so important for the selection of appropriate surgical approach preoperatively. While the risk for recurrence in Warthin's tumours which treated by surgically is approxi-

mately 2%, the risk for local recurrence in pleomorphic adenomas which treated in the same manner was reported as approximately 85% (10). Additionally, surgical treatment of pleomorphic adenomas have to be more aggressive because of the risk of malignant transformation. In many cases, probability of relapsing and necessity of determining the relationship between mass and facial nerve, would be imminent to the diagnostic imaging methods for making treatment method definite and modifying surgical approach (11).

Recently, with some techniques based on MRI that is commonly used in the diagnosis of parotid gland tumors and which has advantages such as excellent soft tissue resolution, multiplanar imaging ability, not included x-ray that is harmful to the health had been evaluated for distinguishing between benign and malignant parotid gland tumors. The morphological evaluation of the tumors and staging the diseases are most important utility of MRI that as a noninvasive technique contrast to the fine needle aspiration biopsy (FNAB). However, distinguishing between benign or malignant parotid gland tumours was described as 'difficult' by conventional MRI (12,13). Besides, distinguishing of many benign and malignant lesions by FNAB had been reported as difficult, even impossible (14,15). King et al. tested proton magnetic resonance spectroscopy imaging (1H-MRS) to make differential diagnosis for parotid gland tumors (16). However, 1H-MRS couldn't be performed in small tumors because of the risk of contaminating the signals by adjacent structures. As a result of recent studies, the DWI which is the techniques based on MRI, seems having the highest potential to detect different histologic subtypes of parotid gland tumors noninvasively (17-21).

ADC value is affected by morphology of tumour including ratio of nucleus/cytoplasm and cellular density (22) and an inverse correlation between the ADC value and tumor cellularity has been shown in experimental models, and this has been clinically validated (23-25). The studies that compare ADC values and histopathological results strongly show that denser cellularity is interested in restricted diffusion. However, features of extracellular compartment except cellularity affect to the ADC values too. As a result, tissue contrast of tumour is mostly affected by degenerative alterations in interstitial tissue such as the degree of differentiation of tumor cells, presence or absence of necrosis and cystic component, myxomatous alterations and also diversity of tumor tissue components. Motoori et al. reported the importance of the distinction of myxoid tissue by MRI to differentiate between pleomorphic adenoma and malignant tumor (26).

Besides, in another study, they also reported that the high ADC values in pleomorphic adenomas were related to myxoid and/or chondroid matrix (20). At the same time, the highest ADC value had been determined at pleomorphic adenomas in the parotid gland tumours. In many reports that ADC values had been calculated, it is mentioned that calculation of ADC values might be helpful for differentiating parotid gland tumours (17-21).

In this study, we found that highest ADC values belong to pleomorphic adenoma including myxoid and/or chondroid matrix ($2.10 \pm 0.26 \times 10^{-3} \text{ mm}^2/\text{sec}$). The mean ADC values of pleomorphic adenomas were significantly higher than that of Warthin's tumors, basal cell adenomas and cystic lesions in our study. And also ADC values of the patients who have pleomorphic adenoma were significantly higher than the malignant one.

Additionally, we could differentiate pleomorphic adenoma from other all benign/malignant tumours, just Warthin's tumours and just malignant tumours in high sensitivity and specificity with cutoff ADC values that were determined by using ROC curve analysis for characterizing of parotid gland tumours. The cutoff ADC value for distinguishing the pleomorphic adenoma from these parotid masses was $1.60 \times 10^{-3} \text{ mm}^2/\text{sec}$, with sensitivity of 94.7% (18/19, 95% CI) and specificity of 100% (22/22, %95 CI). Thus, the ADC values of pleomorphic adenomas were not overlapped with nearest ADC value of benign or malignant tumour. The ADC values that over this result were shown consistency with histopathologi-

cal results. As a result of our study, the most seen parotid gland mass was pleomorphic adenoma that was similar to the literature.

The morphologic features of Warthin's tumor mimic malignant tumors (27). In a study performed by Ikeda et al. (28), ADC values of Warthin's tumors ($0.96 \pm 0.13 \times 10^{-3} \text{ mm}^2/\text{sec}$) were significantly lower than malignant lesions ($1.19 \pm 0.19 \times 10^{-3} \text{ mm}^2/\text{sec}$). However, ADC value of Warthin's tumors ($0.72 \times 10^{-3} \text{ mm}^2/\text{s} - 1.17 \times 10^{-3} \text{ mm}^2/\text{s}$) show variability as overlapping malignant ones ($0.79 \times 10^{-3} \text{ mm}^2/\text{s} - 1.65 \times 10^{-3} \text{ mm}^2/\text{s}$). Yerli et al. reported that ADC values of Warthin's tumor ($0.97 \pm 0.16 \times 10^{-3} \text{ mm}^2/\text{sec}$) didn't have significant difference with malignant lesions ($0.97 \pm 0.16 \times 10^{-3} \text{ mm}^2/\text{sec}$) in a similar study (29). But, they had been thought that this is related to having large number of lymphoma. Furthermore, Yerli et al. reported that the combination of MRI and DWI with ADC calculation might have a similar diagnostic value for determining specific histological types when compared with FNAB in else study (30).

In the results of our study, ADC values of Warthin's tumor were $0.94 \pm 0.05 \times 10^{-3} \text{ mm}^2/\text{sec}$ that supported to the studies that was performed by Ikeda et al. and Yerli et al. ADC values of Warthin's tumours ($0.88 \times 10^{-3} \text{ mm}^2/\text{sec} - 1.0 \times 10^{-3} \text{ mm}^2/\text{sec}$) were varied by not overlapping with ADC values of malignant tumors ($1.03 \times 10^{-3} \text{ mm}^2/\text{s} - 1.53 \times 10^{-3} \text{ mm}^2/\text{s}$) similar to that was reported by Ikeda et al. And also the ADC values of Warthin's tumours were invented as significantly lower than malignant tumors in our study. In contrast to the literature, we could differentiate Warthin's tumour from malignant tumours by measuring ADC values that was similar to the pleomorphic adenoma. There were 4 Warthin's tumor in our study and we thought that our study has to be supported by further studies with larger populations.

In the previous studies that was reported by Ikeda (28) and Yerli et al. (29), ADC values for malignant tumours were reported as $1.19 \pm 0.19 \times 10^{-3} \text{ mm}^2/\text{sec}$ and $1.04 \pm 0.35 \times 10^{-3} \text{ mm}^2/\text{sec}$, respectively. Making definitive diagnosis is not possible in everytime just with conventional MRI sequences and the ADC values alone are not sufficient to differentiate benign from malignant salivary gland tumors (30,31).

Because of the small number of types of malignant lesion in our study, they were not compared among themselves according to the ADC values and there was a pronounced overlapping between ADC values. The mean ADC values

of malignant tumours in our study was $1.13 \pm 0.13 \times 10^{-3}$ mm²/sec; and also the ADC value range was changed between 1.02×10^{-3} mm²/sec and 1.15×10^{-3} mm²/sec when we excluded the adenoid cystic carcinoma that had high ADC value. The mean ADC values of malignant tumours were significantly lower than pleomorphic adenoma and significantly higher than Warthin's tumours in our study. Malignant parotid tumours were distinguished from Warthin's tumour by cutoff ADC value as 1.01×10^{-3} mm²/sec, with sensitivity of 92.3% (12/13, 95% CI) and specificity of 100% (4/4, 95% CI) according to ROC curve analysis. We found that the most common malignant parotid tumour was secondary tumours different from the literature.

Although the variety of malignant tumour subgroups was enough in our study, the number of each one was still limited. However parotid gland tumours are uncommon. Although we reached similar results in our examination like many previous studies, the main limitation of our study was the presence of insufficient number of tumours particularly in malignant tumours and Warthin's tumour. Therefore, the ADC values for each subtypes of parotid gland tumours may show variability if the further studies can be executed with a large number of patients.

In conclusion, with ADC values, we differentiated pleomorphic adenomas, Warthin tumours and malignant tumours each other which are the most often parotid gland tumours. The calculation ADC values supply a helpful tool for making differential diagnosis of parotid gland tumours. But, the DWI that doesn't inform enough anatomical knowledge has to be performed together with routine MRI sequences combined with morphological analysis.

REFERENCES

1. Le Bihan D, Breton E, Lallemand D, Aubin ML, Vignaud J, Laval-Jeantet M. Separation of diffusion and perfusion in intravoxel incoherent motion MR imaging. *Radiology* 1988; 168: 497-505.
2. Herneth AM, Guccione S, Bednarski M. Apparent diffusion coefficient: a quantitative parameter for in vivo tumor characterization. *Eur J Radiol* 2003; 45: 208-13.
3. Batori M, Mariotta G, Giovannone G, Casella G, Casella MC. Warthin's tumor of parotid gland: treatment of a retroneural lesion by enucleation. *Eur Rev Med Pharmacol Sci* 2002; 6: 105-11.
4. Zhang Y, Chen J, Shen J, Zhong J, Ye R, Liang B. Apparent diffusion coefficient values of necrotic and solid portion of lymph nodes: differential diagnostic value in cervical lymphadenopathy. *Clin Radiol*. 2013; 68(3): 224-31.
5. Chawla S, Kim S, Dougherty L, et al. Pretreatment diffusion-weighted and dynamic contrast-enhanced MRI for prediction of local treatment response in squamous cell carcinomas of the head and neck. *AJR Am J Roentgenol* 2013; 200(1): 35-43.
6. Baltzer PA, Benndorf M, Dietzel M, Gajda M, Camara O, Kaiser WA. Sensitivity and specificity of unenhanced MR mammography (DWI combined with T2-weighted TSE imaging, ueMRM) for the differentiation of mass lesions. *Eur Radiol* 2010; 20: 1101-10.
7. Öztekin O, Ozan E, Hilal Adıbelli Z, Ünal G, Abali Y. SSH-EPI diffusion-weighted MR imaging of the spine with low b values: is it useful in differentiating malignant metastatic tumor infiltration from benign fracture edema? *Skeletal Radiol* 2009; 38: 651-8.
8. Nagata S, Nishimura H, Uchida M, Hayabuchi N. Diffusion-weighted MR Imaging in Musculoskeletal Radiology. *Japanisch-Deutsche Medizinische Berichte* 2005; 50: 640-51.
9. Koh DM, Collins DJ. Diffusion-weighted MRI in the body: applications and challenges in oncology. *Am J Roentgenol* 2007; 188: 1622-35.
10. Donovan DT, Conley JJ. Capsular significance in parotid tumor surgery: reality and myths of lateral lobectomy. *Laryngoscope* 1984; 94: 324-9.
11. Friedman M, Rice DH, Spiro RH. Difficult decisions in parotid surgery. *Otolaryngol Clin North Am* 1986; 19: 637-45.
12. Joe VQ, Westesson PL. Tumors of the parotid gland: MR imaging characteristics of various histologic types. *AJR Am J Roentgenol* 1994; 163: 433-8.
13. Takashima S, Sone S, Takayama F, et al. Assessment of parotid masses: which MR pulse sequences are optimal? *Eur J Radiol* 1997; 24: 206-15.
14. Das DK, Petkar MA, Al-Mane NM, Sheikh ZA, Mallik MK, Anim JT. Role of fine needle aspiration cytology in the diagnosis of swellings in the salivary gland regions: a study of 712 cases. *Med Princ Pract* 2004; 13: 95-106.
15. Behzatoğlu K, Bahadır B, Kaplan HH, Yücel Z, Durak H, Bozkurt ER. Fine needle aspiration biopsy of the parotid gland. Diagnostic problems and 2 uncommon cases. *Acta Cytol* 2004; 48: 149-54.
16. King AD, Yeung DK, Ahuja AT, et al. Salivary gland tumors at in vivo proton MR spectroscopy. *Radiology* 2005; 237: 563-9.
17. Eida S, Sumi M, Sakihama N, Takahashi H, Nakamura T. Apparent diffusion coefficient mapping of salivary gland tumors: prediction of the benignancy and malignancy. *AJNR Am J Neuroradiol* 2007; 28: 116-21.
18. Habermann CR, Gossrau P, Graessner J, et al. Diffusion-weighted echo-planar MRI: a valuable tool for differentiating primary parotid gland tumors? *Rofo* 2005; 177: 940-5.
19. Yoshino N, Yamada I, Ohbayashi N, et al. Salivary glands and lesions: evaluation of apparent diffusion coefficients with split-echo diffusion-weighted MR imaging--initial results. *Radiology* 2001; 221: 837-42.

20. Motoori K, Yamamoto S, Ueda T, *et al.* Inter- and intratumoral variability in magnetic resonance imaging of pleomorphic adenoma: an attempt to interpret the variable magnetic resonance findings. *J Comput Assist Tomogr* 2004; 28: 233-46.
21. Habermann CR, Arndt C, Graessner J, *et al.* Diffusion-Weighted Echo-Planar MR Imaging of Primary Parotid Gland Tumors: Is a Prediction of Different Histologic Subtypes Possible? *AJNR Am J Neuroradiol* 2009; 30(3): 591-6.
22. Szafer A, Zhong J, Anderson AW, Gore JC. Diffusion-weighted imaging in tissues: theoretical models. *NMR Biomed* 1995; 8: 289-96.
23. Chenevert TL, Meyer CR, Moffat BA, *et al.* Diffusion MRI: a new strategy for assessment of cancer therapeutic efficacy. *Mol Imaging* 2002; 1: 336-43.
24. Ross BD, Moffat BA, Lawrence TS, *et al.* Evaluation of cancer therapy using diffusion magnetic resonance imaging. *Mol Cancer Ther* 2003; 2: 581-7.
25. Guo AC, Cummings TJ, Dash RC, Provenzale JM. Lymphomas and high-grade astrocytomas: comparison of water diffusibility and histologic characteristics. *Radiology* 2002; 224: 177-83.
26. Motoori K, Iida Y, Nagai Y, *et al.* MR imaging of salivary duct carcinoma. *AJNR Am J Neuroradiol* 2005; 26: 1201-6.
27. Minami M, Tanioka H, Oyama K, *et al.* Warthin tumor of the parotid gland: MR-pathologic correlation. *AJNR Am J Neuroradiol* 1993; 14: 209-14.
28. Ikeda M, Motoori K, Hanazawa T, *et al.* Warthin tumor of the parotid gland: diagnostic value of MR imaging with histopathologic correlation. *AJNR Am J Neuroradiol* 2004; 25: 1256-62.
29. Yerli H, Agildere M, Aydin E, *et al.* Value of apparent diffusion coefficient calculation in the differential diagnosis of parotid gland tumors. *Acta Radiol* 2007; 9: 980-7.
30. Yerli H, Aydin E, Haberal N, Harman A, Kaskati T, Alibek S. Diagnosing common parotid tumours with magnetic resonance imaging including diffusion-weighted imaging vs fine-needle aspiration cytology: a comparative study. *Dentomaxillofac Radiol* 2010; 39(6) :349-55.
31. Ikeda K, Katoh T, Ha-Kawa SK, Iwai H, Yamashita T, Tanaka Y. The usefulness of MR in establishing the diagnosis of parotid pleomorphic adenoma. *AJNR Am J Neuroradiol* 1996; 17: 555-9.